



A multicompartment mathematical model to study the dynamic behaviour of COVID-19 using vaccination as control parameter

Sonu Kurmi · Usha Chouhan

Received: 11 December 2021 / Accepted: 31 May 2022 / Published online: 13 June 2022
© The Author(s), under exclusive licence to Springer Nature B.V. 2022

Abstract To analyse novel coronavirus disease (COVID-19) transmission in India, this article provides an extended SEIR multicompartment model using vaccination as a control parameter. The model considers eight classes of infection: susceptible (S), vaccinated (V), exposed (E), asymptomatic infected (A), symptomatic infected (I), isolated (J), hospitalised (H), recovered (R). To begin, a mathematical study is performed to demonstrate the suggested model's uniform boundedness, epidemic equilibrium, and basic reproduction number. The findings indicate that if, $R_0 < 1$, the disease-free equilibrium is locally asymptotically stable; but, if, $R_0 > 1$ the equilibrium is unstable. Secondly, we examine the effect on those who have received vaccinations with what are deemed optimal values. The suggested model is numerically simulated using MATLAB 14.0, and the results confirm the capacity of the proposed model to provide an accurate forecast of the progress of the epidemic in India. Finally, we examine the impact of immunisation on COVID-19 dissemination.

Keywords COVID-19 · Mathematical model · Vaccination · Sensitivity analysis · Numerical simulation

Mathematics Subject Classification MSC 34-04

1 Introduction

The world is currently grappling with a novel infectious disease, coronavirus disease. In February 2020, the World Health Organization (WHO) termed this disease COVID-19 [1]. The disease initially manifested itself in December 2019 at the Huanan seafood market in Wuhan, Hubei, China. Nowadays, the number of affected people is growing daily. COVID-19 was declared a global pandemic by the WHO on March 11, 2020 [2]. As of September 17, 2021, about 226 million confirmed cases of COVID-19 had been reported to WHO, including over 4 million deaths [3]. India's first reported COVID-19 case occurred in Kerala on January 30, 2020, when a 20-year-old lady returned to India from Wuhan, China [4]. As of September 17, 2021, about 33 million confirmed cases of COVID-19 had been detected in India, with over 444 thousand deaths reported to the WHO [5].

Individuals spread COVID-19 through their respiratory droplets after coming into contact with contaminated objects or sick individuals. Social separation is used to keep people apart and to put an end to overcrowded social events. The symptoms of all

S. Kurmi (✉) · U. Chouhan
Department of Mathematics, Bioinformatics and Computer Applications, Maulana Azad National Institute of Technology, Bhopal, Madhya Pradesh, India
e-mail: sk.193104001@manit.ac.in

U. Chouhan
e-mail: chouhanu@manit.ac.in

coronavirus patients are identical, including respiratory difficulties, fever, and a dry cough. Numerous shops, supermarkets, department stores, and public areas were closed to prevent individuals from encountering one another, and various countries implemented lockdown procedures to limit the spread of the disease. During the COVID-19 pandemic, some countries employed non-pharmaceutical interventions (NPIs) such as mask use, social isolation, and appropriate sanitation to help prevent the virus spread. This process contributes to the slowing but not a complete cessation of the spread. However, vaccination is being initiated in order to combat COVID-19.

Mathematical models are researched to better understand infectious disease behaviour and to forecast transmission dynamics for the purpose of regulating and planning measures [6–8]. Numerous model-based studies have effectively captured the worldwide dynamics of the corresponding infectious illness throughout the history of literature [9–16]. Significant research has been conducted or is currently being conducted to uncover COVID-19 using appropriate mathematical models. Ndairou et al. [17] proposed a compartmental mathematical model for the spread of the COVID-19 disease, focusing on the transmissibility of super-spreaders among individuals. Mandal et al. [18] develop a mathematical model wherein they include a quarantine class and government intervention methods to help minimise disease spread. In a separate recent study, Prathumwan et al. [19] developed a mathematical model for projecting the COVID-19 outbreak's propagation in order to explore the impacts of quarantined, hospitalised, and latent class people. Using a deterministic compartmental model, Biswas et al. [20] investigated the propagation of COVID-19 and determined model parameters using data from an active epidemic in India. In their work, Gumel et al. [21] demonstrate how several main non-pharmaceutical COVID-19 therapies might be included in the epidemic model. Additionally, a short summary of different models used to explore the dynamics of COVID-19 is given, covering agent-based, network, and statistical models. In another recent work, Ghostine et al. [22] have proposed an enhanced SEIR model including a vaccination compartment to mimic the spread of a new coronavirus epidemic in Saudi Arabia. Das et al. [23] developed a mathematical model including comorbidity in order to investigate the transmission dynamics of COVID-19.

Das et al. [24] proposed and explored a mathematical framework to study the transmission dynamics of COVID-19 with comorbidity. Yu et al. [25] proposed compartmental model to study the development of COVID-19 in India after relaxing control. Hu et al. [26] assessed the controllability of spread of COVID-19 in different stages based on proposed compartmental model.

Due to the fact that the nature and destruction of COVID-19 are dependent on a variety of system parameters (such as personal immunity, history of travel to a COVID-19 pandemic country, and maintaining the required hygiene), we cannot use a single model to describe the entire disease system worldwide. While adding richness and complexity to models might improve their accuracy, it also complicates their mathematics. To combat COVID-19 as a pandemic, appropriate immunisation efforts utilising NPIs must be developed. To accomplish this, coupled fundamental tactics are unavoidably necessary under optimal control strategies to eradicate COVID-19 as an infectious disease at the lowest possible cost of vaccination. The primary objective of this effort is to determine the optimal control strategy for COVID-19 infection using NPIs and vaccination. Consideration of asymptomatic infected, symptomatic infected, and vaccination classes in the proposed compartmental model requires an extensive investigation of disease-free equilibrium points. We have assumed the model parameters and evaluated the adequate reproduction number. We have done model fitting, parameter estimation, and validation of the model.

The following sections comprise the manuscript for this article: Sect. 2 introduces the model formulation. Section 3 conducts a qualitative study of the model. We examine the positivity and boundedness of solutions in Sect. 3.1, we study the positivity and boundedness of solutions. We compute the disease-free equilibrium E_0 , in Sect. 3.2. Following that, in Sect. 3.3, we also compute the basic reproduction number R_0 of the COVID-19 system model. In Sect. 3.4, we examine the local stability of the disease-free equilibrium in terms of R_0 . Sect. 4 formulates and solves an optimal control problem analytically. Section 5 illustrates the model's utility through numerical simulation; Sect. 5.1 illustrates the fixed control parameter. Section 5.2 discusses the sensitivity of the reproduction number, R_0 , to the parameters of the model system. In Sect. 5.3, we discussed the bifurcation diagram. The numerical

simulation of the optimal control problem is shown in Sect. 5.4. Parameter-estimation, model fitting and model validation is discussed in Sect. 5.5. The conclusion concludes with Sect. 6.

2 The proposed mathematical model

In this section, we shall study the transmission mechanism of COVID-19 using a deterministic compartmental model. To formulate the mathematics model, we have divided the total population $\mathcal{X}(t)$ into eight mutually exclusive compartments based on their disease status namely: susceptible $\mathcal{S}(t)$, vaccinated $\mathcal{V}(t)$, exposed $\mathcal{E}(t)$, asymptomatic infected $\mathcal{A}(t)$, symptomatic infected $\mathcal{I}(t)$, isolated $\mathcal{J}(t)$, hospitalised $\mathcal{H}(t)$ and recovered $\mathcal{R}(t)$.

Some of the classes are discussed in more detail here. In the exposed class $\mathcal{E}(t)$, we consider those individuals of the susceptible and vaccinated classes who have had sufficient interaction with the infected individuals or contaminated surfaces or objects. There is an incubation period and a latency period. The incubation period is the period between exposure and the onset of clinical symptoms. The latent period is the period between exposure and communicability, which may be shorter or longer than the incubation period. In COVID-19, the latent period is shorter than the incubation period [27]. This fact leads us to make another two classes from the exposed class, namely asymptomatic infected $\mathcal{A}(t)$ and symptomatic infected $\mathcal{I}(t)$. Asymptomatic infected class $\mathcal{A}(t)$ contains those individuals of the exposed class who lie between the latent period and the incubation period, and symptomatic infected class $\mathcal{I}(t)$, contains those individuals of the exposed class who lie between the incubation period and infection period.

The mixing of individual hosts is homogeneous, and thus the law of the mass action holds. The rate of transfer from a compartment is in proportion to the population size of the compartment. There is no loss of immunity and no possibility of reinfection. Our model assumes that vaccinated individuals have to be separated into a vaccinated class $\mathcal{V}(t)$. Π is the birth/recruitment rate into the population, μ is the per capita natural death rate, β is the per capita transmission rate, α is the constant of vaccination, ξ is the transfer rate of vaccinated individuals to get exposed or called vaccine inefficacy, ϵ is the transfer rate of exposed indi-

viduals to asymptomatic infected, δ is the transfer rate of exposed individuals to symptomatic infected, θ is the rate of asymptomatic infected individuals to become isolated, λ is the rate of symptomatic infected individuals become hospitalised. η_a, η_i and η_j are the disease-induced death rates of asymptomatic infected, symptomatic infected, and isolated infected, respectively, and ρ_a, ρ_i, ρ_j and ρ_h are the recovery rates of asymptomatic infected, symptomatic infected, isolated infected, and hospitalised individuals, respectively.

We provide in Fig. 1 the flow diagram of the COVID-19 transmission model under the aforementioned assumptions, which illustrates the many interactions between classes. The inward and outward arrows indicate the population increasing and decreasing, accordingly.

According to the conditions outlined above and the flow diagram (Fig. 1), the transmission of the virus is governed by the following system of ODEs:

$$\begin{aligned}
 \dot{\mathcal{S}} &= \Pi - \beta\mathcal{S}(\mathcal{A} + \mathcal{I}) - \alpha u(t)\mathcal{S} - d\mathcal{S} \\
 \dot{\mathcal{V}} &= \alpha u(t)\mathcal{S} - \beta\xi\mathcal{V}(\mathcal{A} + \mathcal{I}) - d\mathcal{V} \\
 \dot{\mathcal{E}} &= \beta\mathcal{S}(\mathcal{A} + \mathcal{I}) + \beta\xi\mathcal{V}(\mathcal{A} + \mathcal{I}) - (\epsilon + \delta + d)\mathcal{E} \\
 \dot{\mathcal{A}} &= \epsilon\mathcal{E} - (\theta + \eta_a + d + \rho_a)\mathcal{A} \\
 \dot{\mathcal{I}} &= \delta\mathcal{E} - (\kappa + \lambda + \eta_i + d + \rho_i)\mathcal{I} \\
 \dot{\mathcal{J}} &= \theta\mathcal{A} + \kappa\mathcal{I} - (\mu + \rho_j + \eta_j + d)\mathcal{J} \\
 \dot{\mathcal{H}} &= \lambda\mathcal{I} + \mu\mathcal{J} - (\rho_h + \eta_h + d)\mathcal{H} \\
 \dot{\mathcal{R}} &= \rho_a\mathcal{A} + \rho_i\mathcal{I} + \rho_j\mathcal{J} + \rho_h\mathcal{H} - d\mathcal{R}
 \end{aligned} \tag{1}$$

The initial condition of system (1) is $\mathcal{S}(0) \geq 0, \mathcal{V}(0) \geq 0, \mathcal{E}(0) \geq 0, \mathcal{A}(0) \geq 0, \mathcal{I}(0) \geq 0, \mathcal{J}(0) \geq 0, \mathcal{H}(0) \geq 0$, and $\mathcal{R}(0) \geq 0$. The description of the state variables, control variables, and parameters used in the model with values is provided in Table 1.

3 Analysis of the model for fixed control

In this section, we analyse the model for fixed control, i.e. $u(t)$ must be constant. Therefore, αu is also constant, so without loss of generality, we replace αu with another constant α and carry out the analysis part.

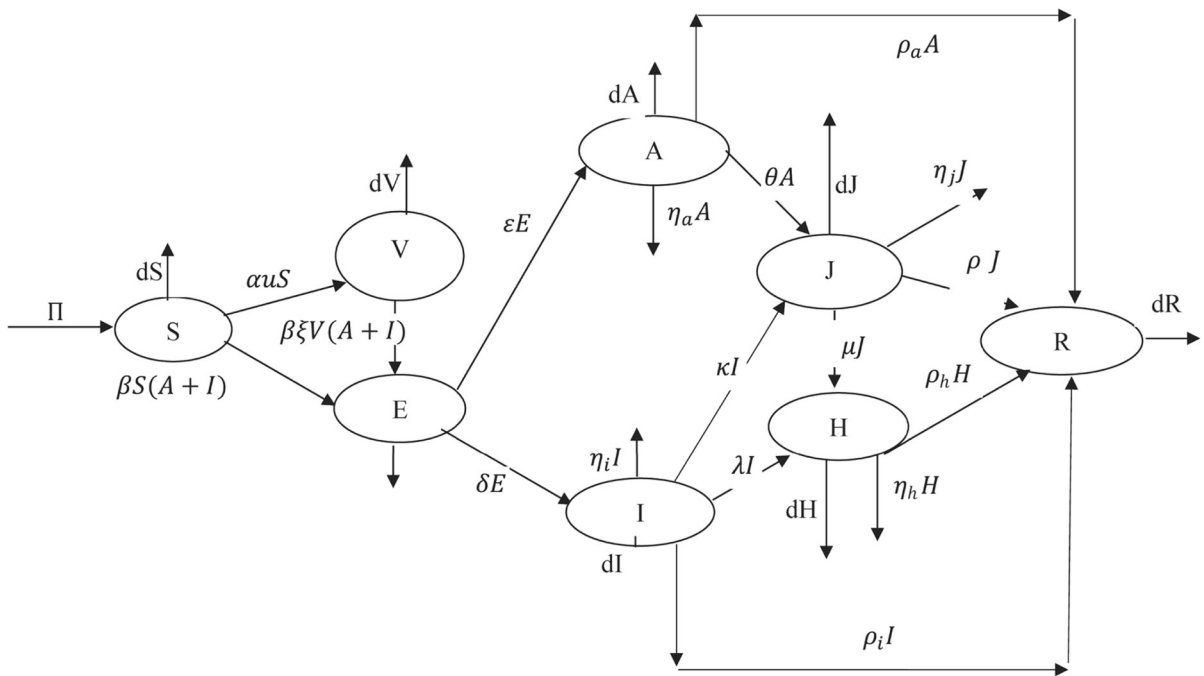


Fig. 1 Pictorial scenario of model (1). The flowchart shows the interaction of different stages of individuals in the model: susceptible (S), vaccinated (V), exposed (E), asymptomatic infected

(A), symptomatic infected (I), isolated (J), hospitalised (H), recovered (R)

3.1 Positivity and boundedness of solutions

Theorem 1 *The solutions of system (1) are nonnegative and uniformly bounded.*

Proof We assume that

$$\begin{aligned} \mathcal{X} &= S + V + E + A + I + J + H + R. \\ \Rightarrow \dot{\mathcal{X}} &= \dot{S} + \dot{V} + \dot{E} + \dot{A} + \dot{I} + \dot{J} + \dot{H} + \dot{R} \\ \Rightarrow \dot{\mathcal{X}} + d\mathcal{X} &= \Pi - \eta_a A - \eta_i I - \eta_j J - \eta_h H \\ \Rightarrow \mathcal{X} + d\mathcal{X} &\leq \Pi \\ \Rightarrow \mathcal{X} &\leq \frac{\Pi}{d}(1 - e^{-dt}) + \mathcal{X}_0 e^{-dt}. \end{aligned}$$

Now for $t \rightarrow \infty$

$$0 < \mathcal{X} \leq \frac{\Pi}{d}.$$

Hence, all the solution system (1) that are initiating in $\{\mathbb{R}_+^8\}$ are confined in the region

$$\{\mathcal{X} \in \mathbb{R}_+^8 : 0 \leq \mathcal{X} < \frac{\Pi}{d} + \epsilon\}$$

for any $\epsilon > 0$ and $t \rightarrow \infty$. □

3.2 The disease-free equilibrium E_0

The disease-free equilibrium E_0 of system (1) is obtained by setting all derivatives to 0 with $\mathcal{A} = 0$ and $\mathcal{I} = 0$ and solving all variables, that yields to:

$$E_0 = \left(\frac{\Pi}{\alpha + d}, \frac{\Pi \alpha}{d(\alpha + d)}, 0, 0, 0, 0, 0, 0 \right). \quad (2)$$

3.3 The basic reproduction number R_0

The basic reproduction number R_0 is the most crucial epidemiological parameter for determining the nature of the disease. It is used to measure the transmission potential of an infectious disease. Additionally, it is essential for disease management and transmission. In epidemiology, the basic reproduction number, R_0 , (sometimes called the basic reproduction ratio or basic reproductive rate), is the average number of new infections caused by a single infected individual at the time t in the susceptible populations. Van den Driessche and Watmough [28] proposed a method for determining the basic reproduction number, named

Table 1 Description and values of the parameters used in the model (1)

Parameters	Description of parameters	Value	Source
Π	Recruitment rate to susceptible class	50	Assumed
α	Constant of vaccination	0.9	Assumed
β	Disease transmission rate	0.1	Assumed
ξ	Transfer rate of vaccinated individuals to get exposed	0.01	Assumed
d	Natural death rate	0.2	Assumed
ϵ	Transfer rate of exposed individuals to asymptomatic infected	0.09	Assumed
δ	Transfer rate of exposed individuals to symptomatic infected individuals	0.08	Assumed
θ	Transfer rate of asymptomatic infected individuals becomes isolated	0.95	Assumed
κ	Transfer rate of symptomatic infected individuals to become isolated	0.9	Assumed
λ	Transfer rate of symptomatic infected individuals becomes hospitalised	0.85	Assumed
μ	Transformation rate of isolated individuals to becomes hospitalised	0.2	Assumed
η_a	Disease-induced death rate of asymptomatic infected individuals	0.6	Assumed
η_i	Disease-induced death rate of symptomatic infected individuals	0.8	Assumed
η_j	Disease-induced death rate of isolated infected individuals	0.25	Assumed
η_h	Disease-induced death rate of hospitalised individuals	0.25	Assumed
ρ_a	The recovery rate of asymptomatic infected individuals	0.5	Assumed
ρ_i	The recovery rate of symptomatic infected individuals	0.4	Assumed
ρ_j	The recovery rate of isolated infected individuals	0.4	Assumed
ρ_h	The recovery rate of hospitalised infected individuals	0.25	Assumed
u	Control Variable	0.9	Assumed

the next-generation matrix method. By employing the next-generation matrix approach, we determine the basic reproduction number. \mathcal{E} , \mathcal{A} , \mathcal{I} , \mathcal{J} and \mathcal{H} are the classes that are directly engaged in disease transmission. Therefore, from system (1), we have

$$\begin{aligned}
 \dot{\mathcal{E}} &= \beta S(\mathcal{A} + \mathcal{I}) + \beta \xi \mathcal{V}(\mathcal{A} + \mathcal{I}) - (\epsilon + \delta + d)\mathcal{E} \\
 \dot{\mathcal{A}} &= \epsilon \mathcal{E} - (\theta + \eta_a + d + \rho_a)\mathcal{A} \\
 \dot{\mathcal{I}} &= \delta \mathcal{E} - (\kappa + \lambda + \eta_i + d + \rho_i)\mathcal{I}
 \end{aligned}
 \tag{3}$$

$$\begin{aligned}
 \dot{\mathcal{J}} &= \theta \mathcal{A} + \kappa \mathcal{I} - (\mu + \rho_j + \eta_j + d)\mathcal{J} \\
 \dot{\mathcal{H}} &= \lambda \mathcal{I} + \mu \mathcal{J} - (\rho_h + \eta_h + d)\mathcal{H}
 \end{aligned}$$

Hence, we decompose the right-hand side of system (3) as $\mathfrak{F} - \mathfrak{W}$, where

$$\mathfrak{F} = \begin{pmatrix} \beta S(\mathcal{A} + \mathcal{I}) + \beta \xi \mathcal{V}(\mathcal{A} + \mathcal{I}) \\ 0 \\ 0 \\ 0 \\ 0 \end{pmatrix} \text{ and}$$

$$\mathfrak{V} = \begin{pmatrix} (\epsilon + \delta + d)\mathcal{E} \\ (\theta + \eta_a + d + \rho_a)\mathcal{A} - \epsilon\mathcal{E} \\ (\kappa + \lambda + \eta_i + d + \rho_i)\mathcal{I} - \delta\mathcal{E} \\ (\mu + \rho_j + \eta_j + d)\mathcal{J} - \theta\mathcal{A} - \kappa\mathcal{I} \\ (\rho_h + \eta_h + d)\mathcal{H} - \lambda\mathcal{I} - \mu\mathcal{J} \end{pmatrix}.$$

The Jacobian matrices of \mathfrak{F} and \mathfrak{V} are given by \mathbf{F} and \mathbf{V} , respectively.

$$\tilde{\mathbf{F}} = \frac{\partial \mathfrak{F}}{\partial x_j}(E_0) = \begin{pmatrix} 0 & \frac{\beta\Pi}{d(\alpha+d)}(d + \xi\alpha) & \frac{(d+\xi\alpha)\beta\Pi}{d(\alpha+d)} & 0 & 0 \\ 0 & 0 & 0 & 0 & 0 \\ 0 & 0 & 0 & 0 & 0 \\ 0 & 0 & 0 & 0 & 0 \\ 0 & 0 & 0 & 0 & 0 \end{pmatrix}$$

and

$$\tilde{\mathbf{V}} = \frac{\partial \mathfrak{V}}{\partial x_j}(E_0) = \begin{pmatrix} (\epsilon + \delta + d) & 0 & 0 & 0 & 0 \\ -\epsilon & (\theta + \eta_a + d + \rho_a) & 0 & 0 & 0 \\ -\delta & 0 & \kappa + \lambda + \eta_i + d + \rho_i & 0 & 0 \\ 0 & -\theta & -\kappa & (\mu + \rho_j + \eta_j + d) & 0 \\ 0 & 0 & -\lambda & -\mu & (\rho_h + \eta_h + d) \end{pmatrix}$$

for $x_j = \mathcal{E}, \mathcal{A}, \mathcal{I}, \mathcal{J}$, and \mathcal{H} . Or

$$\tilde{\mathbf{F}} = \begin{pmatrix} 0 & c & c & 0 & 0 \\ 0 & 0 & 0 & 0 & 0 \\ 0 & 0 & 0 & 0 & 0 \\ 0 & 0 & 0 & 0 & 0 \\ 0 & 0 & 0 & 0 & 0 \end{pmatrix} \text{ and } \tilde{\mathbf{V}} = \begin{pmatrix} c_1 & 0 & 0 & 0 & 0 \\ -\epsilon & c_2 & 0 & 0 & 0 \\ -\delta & 0 & c_3 & 0 & 0 \\ 0 & -\theta & -\kappa & c_4 & 0 \\ 0 & 0 & -\lambda & -\mu & c_5 \end{pmatrix}$$

where, $c_1 = \epsilon + \delta + d, c_2 = \theta + \eta_a + d + \rho_a, c_3 = \kappa + \lambda + \eta_i + d + \rho_i, c_4 = \mu + \rho_j + \eta_j + d, c_5 = \rho_h + d$, and $c = \frac{\beta\Pi(\xi\alpha+d)}{d(\alpha+d)}$.

Because the basic reproduction number is equal to the spectral radius of the matrix $\tilde{\mathbf{F}}\tilde{\mathbf{V}}^{-1}$. As a result, we know that the basic reproduction number for the model under consideration is

$$R_0 = \rho(\tilde{\mathbf{F}}\tilde{\mathbf{V}}^{-1}) = \frac{\epsilon c}{c_1 c_2} + \frac{\delta c}{c_1 c_3}. \tag{4}$$

3.4 Stability analysis of the disease-free equilibrium

In this section, we study the stability analysis of the disease-free equilibrium point $E_0 = (\frac{\Pi}{\alpha+d}, \frac{\Pi\alpha}{d(\alpha+d)}, 0, 0, 0, 0, 0)$ whose stability has been investigated in the next theorem.

Theorem 2 *If $R_0 < 1$, then the DFE E_0 is locally asymptotically stable, and it is unstable if $R_0 > 1$.*

Proof The Jacobian matrix corresponding to system 1 at DFE $E_0 (\frac{\Pi}{\alpha+d}, \frac{\Pi\alpha}{d(\alpha+d)}, 0, 0, 0, 0, 0)$ is given as

$$\begin{pmatrix} -(\alpha + d) & 0 & -\beta S^0 & -\beta S^0 & 0 & 0 & 0 & 0 & 0 \\ \alpha & -d & 0 & -\beta \xi \mathcal{V}^0 & -\beta \xi \mathcal{V}^0 & 0 & 0 & 0 & 0 \\ 0 & 0 & -(\epsilon + \delta + d) & \beta S^0 + \beta \xi \mathcal{V}^0 & -\beta \xi \mathcal{V}^0 & \beta S^0 + \beta \xi \mathcal{V}^0 & -\beta \xi \mathcal{V}^0 & 0 & 0 & 0 \\ 0 & 0 & \epsilon & -(\theta + \eta_a + d + \rho_a) & 0 & 0 & 0 & 0 & 0 & 0 \\ 0 & 0 & \delta & 0 & -(\kappa + \lambda + \eta_i + d + \rho_i) & 0 & 0 & 0 & 0 & 0 \\ 0 & 0 & 0 & \theta & \kappa & -(\mu + \rho_j + \eta_j + d) & 0 & 0 & 0 & 0 \\ 0 & 0 & 0 & 0 & \lambda & \mu & -(\rho_h + \eta_h + d) & 0 & 0 & 0 \\ 0 & 0 & 0 & \rho_a & \rho_i & \rho_j & \rho_h & -d & 0 & 0 \end{pmatrix}$$

this can also be written as

$$\begin{pmatrix} -(\alpha + d) - \lambda & 0 & 0 & -\beta S^0 & -\beta S^0 & 0 & 0 & 0 \\ \alpha & -d - \lambda & 0 & -\beta \xi V^0 & -\beta \xi V^0 & 0 & 0 & 0 \\ 0 & 0 & -c_1 - \lambda & c & c & 0 & 0 & 0 \\ 0 & 0 & \epsilon & -c_2 - \lambda & 0 & 0 & 0 & 0 \\ 0 & 0 & \delta & 0 & -c_3 - \lambda & 0 & 0 & 0 \\ 0 & 0 & 0 & \theta & \kappa & -c_4 - \lambda & 0 & 0 \\ 0 & 0 & 0 & 0 & \lambda & \mu & -c_5 - \lambda & 0 \\ 0 & 0 & 0 & \rho_a & \rho_i & \rho_j & \rho_h & -d - \lambda \end{pmatrix}$$

Now, the eigenvalues of the above matrix are the roots of the following characteristic equation:

$$\begin{aligned} & -(\alpha + d + \lambda)(-d - \lambda)(-d - \lambda)(-c_5 - \lambda) \\ & (-c_4 - \lambda)[\delta(c_2 + \lambda)c - (c_3 + \lambda)\{(c_1 + \lambda) \\ & (c_2 + \lambda) - \epsilon c\}] = 0 \\ & -(\alpha + d + \lambda)(-d - \lambda)(-d - \lambda)(-c_5 - \lambda)(-c_4 - \lambda) \\ & [-\lambda^3 - \lambda^2(c_1 + c_2 + c_3) - (c_1c_2 + c_2c_3 + c_3c_1 \\ & - \epsilon c - c\delta)\lambda + \lambda cc_2 \\ & + \epsilon cc_3 - c_3c_1c_2] = 0 \\ & -(\alpha + d + \lambda)(-d - \lambda)(-d - \lambda)(-c_5 - \lambda) \\ & (-c_4 - \lambda)[\lambda^3 + (c_1 + c_2 + c_3)\lambda^2 + (c_1c_2 \\ & + c_2c_3 + c_3c_1 - \epsilon c - c\delta)\lambda + c_1c_2c_3(1 - R_0)] = 0 \\ & -(\alpha + d + \lambda)(-d - \lambda)(-d - \lambda)(-c_5 - \lambda) \\ & (-c_4 - \lambda)[\lambda^3 + a_1\lambda^2 + a_2\lambda + a_3] = 0, \end{aligned}$$

where $a_1 = c_1 + c_2 + c_3$, $a_2 = c_1c_2 + c_2c_3 + c_3c_1 - \epsilon c - c\delta$, $a_3 = c_1c_2c_3(1 - R_0)$.

Following that, using the Liénard-Chipart test, we may determine whether all the roots of the characteristic equation are negative or have a negative real part if and only if the following conditions are met:

$$\begin{aligned} a_2 &> 0, \\ a_1a_2 - a_3 &> 0. \end{aligned}$$

To verify the conditions of the Liénard-Chipart test. We rewrite the coefficients a_1 , a_2 , and a_3 of the characteristic polynomial in terms of the basic reproduction number R_0 given by (4).

$$\begin{aligned} a_1 &= c_1 + c_2 + c_3, \\ a_2 &= c_1(1 - R_0)(c_2 + c_3) + \frac{\delta cc_2}{c_3} + \frac{\epsilon cc_3}{c_2} + c_2c_3, \text{ and} \\ a_3 &= c_1c_2c_3(1 - R_0). \end{aligned}$$

Additionally, we compute the following expression in terms of R_0 :

$$\begin{aligned} a_1a_2 - a_3 &= c_1[c_1c_2 + c_2c_3 + c_3c_1 + c_2^2 + c_3^2](1 - R_0) \\ &+ (c_1 + c_2 + c_3) \left(\frac{\delta cc_2}{c_3} + \frac{\epsilon cc_3}{c_2} + c_2c_3 \right). \end{aligned}$$

As a result of the preceding expressions, it is obvious that if, $R_0 < 1$, the second criterion of the Liénard-Chipart test is satisfied, and the disease-free equilibrium is asymptotically stable. When, $R_0 > 1$, we deduce that at least one eigenvalue is positive using Descartes' rule of signs. \square

The epidemiological implication of Theorem 1 is that a tiny intake of COVID-19-infected individuals will not result in a community outbreak if $R_0 < 1$. That is, the disease rapidly dies out (when $R_0 < 1$) if the initial number of infected individuals is in the basin of attraction of the continuum of the DFE (E_0).

4 The optimal control problem

Control strategies are crucial in reducing COVID-19 transmission. It is necessary to develop a strategy that minimises both the number of affected individuals and associated costs. In this aspect, optimal control theory is an extremely useful tool for determining such a policy. Now, we are concentrating on the most effective techniques for combining non-pharmaceutical treatments with the vaccination process in India. The optimal problem is given by introducing time-varying control $u(t)$, representing a fraction of the vaccination process. The objective functional is constructed as follows:

$$J(u) = \int_0^{t_f} [b_1A + b_2I + \frac{b_3}{2}u^2]dt$$

subject to the proposed model (1). The parameters b_1, b_2 , and $b_3 > 0$ corresponds to the weight constraints for the asymptomatic infected, symptomatic

infected, and vaccination, respectively. By using the standard results, we can show that an optimal state exists. Now, we need to find out the value of the optimal control $u^*(t)$ such that

$$J(u^*) = \min J(u),$$

where $\Omega = \{u \mid 0 \leq u \leq 1, \text{ Lebesgue integral}\}$.

Here, we use the Pontryagin’s maximum principle to derive the necessary conditions for our optimal and corresponding states. The Lagrangian is given by

$$L(\mathcal{V}, \mathcal{A}, \mathcal{I}, u) = b_1\mathcal{A} + b_2\mathcal{I} + \frac{b_3}{2}u^2.$$

The Hamiltonian is defined as follows

$$\begin{aligned} \mathbb{H}(\mathcal{V}, \mathcal{A}, \mathcal{I}, u, \lambda_1, \lambda_2, \lambda_3, \lambda_4, \lambda_5, \lambda_6, \lambda_7, \lambda_8) \\ = L(\mathcal{V}, \mathcal{A}, \mathcal{I}, u) + \lambda_1\dot{\mathcal{S}} \\ + \lambda_2\dot{\mathcal{V}} + \lambda_3\dot{\mathcal{E}} + \lambda_4\dot{\mathcal{A}} + \lambda_5\dot{\mathcal{I}} \\ + \lambda_6\dot{\mathcal{J}} + \lambda_7\dot{\mathcal{H}} + \lambda_8\dot{\mathcal{R}}. \end{aligned}$$

Or

$$\begin{aligned} \mathbb{H} = & \left(b_1\mathcal{A} + b_2\mathcal{I} + \frac{b_3}{2}u^2 \right) + \lambda_1(\Pi \\ & - \beta\mathcal{S}(\mathcal{A} + \mathcal{I}) - \alpha u\mathcal{S} - d\mathcal{S}) \\ & + \lambda_2(\alpha u\mathcal{S} - \beta\xi\mathcal{V}(\mathcal{A} + \mathcal{I}) - d\mathcal{V}) \\ & + \lambda_3(\beta\mathcal{S}(\mathcal{A} + \mathcal{I}) + \beta\xi\mathcal{V}(\mathcal{A} + \mathcal{I}) - c_1\mathcal{E}) \\ & + \lambda_4(\epsilon\mathcal{E} - c_2\mathcal{A}) + \lambda_5(\delta\mathcal{E} - c_3\mathcal{I}) \\ & + \lambda_6(\theta\mathcal{A} + \kappa\mathcal{I} - c_4\mathcal{J}) \\ & + \lambda_7(\lambda\mathcal{I} + \mu\mathcal{J} - c_5\mathcal{H}) + \lambda_8(\rho_a\mathcal{A} \\ & + \rho_i\mathcal{I} + \rho_h\mathcal{H} - d\mathcal{R}). \end{aligned}$$

For the optimal control $u^*(t)$, there exists adjoint variables corresponding to the states variables $\mathcal{S}, \mathcal{V}, \mathcal{E}, \mathcal{A}, \mathcal{I}, \mathcal{J}, \mathcal{H}$, and \mathcal{R} .

$$\begin{aligned} \dot{\lambda}_1(t) = & -\frac{\partial\mathbb{H}}{\partial\mathcal{S}} = -[\lambda_1(-\beta(\mathcal{A} + \mathcal{I}) - \alpha u - d) \\ & + \lambda_2\alpha u + \lambda_3\beta(\mathcal{A} + \mathcal{I})] \end{aligned}$$

$$\begin{aligned} \dot{\lambda}_2(t) = & -\frac{\partial\mathbb{H}}{\partial\mathcal{V}} = -[\lambda_2(-\beta\xi(\mathcal{A} + \mathcal{I}) - d) \\ & + \lambda_3(\beta\xi(\mathcal{A} + \mathcal{I}))] \end{aligned}$$

$$\dot{\lambda}_3(t) = -\frac{\partial\mathbb{H}}{\partial\mathcal{E}} = -[-\lambda_3c_1 + \epsilon\lambda_4 + \delta\lambda_5]$$

$$\begin{aligned} \dot{\lambda}_4(t) = & -\frac{\partial\mathbb{H}}{\partial\mathcal{A}} = -[b_1 - \lambda_1\beta\mathcal{S} - \lambda_2\beta\xi\mathcal{V} \\ & + \lambda_3(\beta\mathcal{S} + \beta\xi\mathcal{V}) - c_2\lambda_4 + \theta\lambda_6 + \rho_a\lambda_8] \end{aligned}$$

$$\begin{aligned} \dot{\lambda}_5(t) = & -\frac{\partial\mathbb{H}}{\partial\mathcal{I}} = -[b_2 - \lambda_1\beta\xi\mathcal{V} + \lambda_3\beta\mathcal{S} \\ & + \lambda_4\beta\xi\mathcal{V} - c_3\lambda_5 + \kappa\lambda_6 + \lambda\lambda_7 + \rho_i\lambda_8] \end{aligned}$$

$$\dot{\lambda}_6(t) = -\frac{\partial\mathbb{H}}{\partial\mathcal{J}} = -[c_4\lambda_6 + \mu\lambda_7 + \lambda_8\rho_h]$$

$$\dot{\lambda}_7(t) = -\frac{\partial\mathbb{H}}{\partial\mathcal{H}} = -[-c_5\lambda_5 + \lambda_8\rho_h]$$

$$\dot{\lambda}_8(t) = -\frac{\partial\mathbb{H}}{\partial\mathcal{R}} = d\lambda_8$$

where the adjoint variables satisfy the transversality conditions $\lambda_1(t_f) = 0, \lambda_2(t_f) = 0, \lambda_3(t_f) = 0, \lambda_4(t_f) = 0, \lambda_5(t_f) = 0, \lambda_6(t_f) = 0, \lambda_7(t_f) = 0, \lambda_8(t_f) = 0$.

We minimise the Hamiltonian concerning the control variable $u^*(t)$.

$$\begin{aligned} \frac{\partial\mathbb{H}}{\partial u} = & b_3u - \alpha\lambda_1\mathcal{S} + \alpha\lambda_2\mathcal{S} = 0 \\ \Rightarrow u^* = & \frac{\alpha\mathcal{S}(\lambda_1 - \lambda_2)}{b_3}. \end{aligned}$$

5 Numerical simulation

5.1 Fixed control

We consider two cases: one with regular vaccination and the other with optimal vaccination control. First, we consider regular vaccination. To simulate our numerical results, we set the parameters for the system (1) that are given in Table 1.

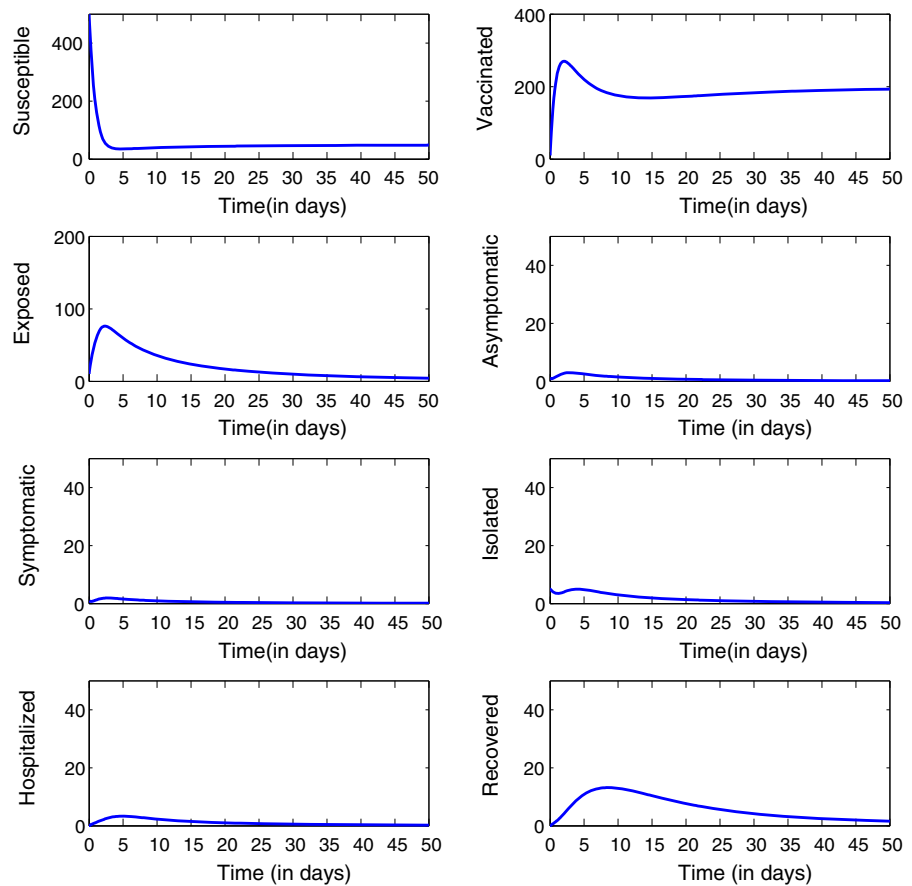
Using the parameters given in Table 1, we calculate the disease-free equilibrium $E_0 = (49.50, 200.49, 0, 0, 0, 0, 0, 0)$ and the basic reproduction number $R_0 = 0.9104$ from equations (2) and (3), respectively. This shows that the system is locally asymptotic stable, and the epidemic outbreak could be controlled. Using these values of parameters and the initial condition as $\mathcal{S}(0) = 500, \mathcal{V}(0) = 10, \mathcal{E}(0) = 10, \mathcal{A}(0) = 1, \mathcal{I}(0) = 1, \mathcal{J}(0) = 5, \mathcal{H}(0) = 0$, and $\mathcal{R}(0) = 0$, we solve our model numerically.

Figure 2 represents that when the basic reproduction number $R_0 < 1$, the system (1) converges to the disease-free equilibrium. Next, when we change the value of u from 0.9 to 0.5, it becomes $R_0 = 1.3902 > 1$, and Fig. 3 shows the variations in all the states of the system (1) when R_0 is greater than unity.

5.2 Sensitivity analysis

Sensitivity analysis for the basic reproduction number, R_0 , tells us, how each parameter involved in the expression of R_0 is essential in disease transmission. It is used

Fig. 2 Simulation results of model (1). The solution trajectory tends towards the disease-free equilibrium (DFE) when $R_0 < 1$



to determine which parameter has a high impact and which has a low impact on the threshold R_0 . Moreover, it has an impact on the dynamics of the proposed model. Sensitivity indices tell us the relative change in the R_0 when a parameter is changed. For performing the sensitivity analysis on R_0 we used the normalised forward sensitivity index of R_0 , concerning the parameters in the expression of R_0 , which is defined as the relative change in the variable for the relative change in its parameters. If the variable is differential for a parameter, then its sensitivity indices are defined as follows.

Definition 1 The normalised forward sensitivity index of a function, $F(x_1, x_2, \dots, x_n)$ for $x_i (1 \leq i \leq n)$, is defined by $\Gamma_{x_i}^F = \frac{\partial F}{\partial x_i} \times \frac{x_i}{F}$.

Therefore, the normalised forward sensitivity index of R_0 for a given parameter θ is given by $\Gamma_{\theta}^{R_0} = \frac{\partial R_0}{\partial \theta} \times \frac{\theta}{R_0}$. The explicit expression of R_0 is given by

$$R_0 = \frac{\epsilon c}{c_1 c_2} + \frac{\delta c}{c_1 c_3},$$

where $c_1 = \epsilon + \delta + d$, $c_2 = \theta + \eta_a + d + \rho a$, $c_3 = \kappa + \lambda + \eta_i + d + \rho_i$, $c_5 = \rho h + \eta_h + d$, and $c = \frac{\beta \Pi (\xi a u + d)}{d(\alpha u + d)}$.

To find sensitivity indices of R_0 , we consider the parameters $\Pi, \beta, \epsilon, \delta, \xi, \alpha, u, d, \theta, \eta_a, \rho_a, \kappa, \lambda, \eta_i$, and λ_i since R_0 is the function of only these parameters. All sensitive indices can be carried out, and expressions are given below.

$$\Gamma_{\epsilon}^{R_0} = \frac{\partial R_0}{\partial \epsilon} \times \frac{\epsilon}{R_0} = -\frac{\epsilon}{c_1} + \frac{c\epsilon}{c_1 c_2 R_0}$$

$$\Gamma_{\delta}^{R_0} = \frac{\partial R_0}{\partial \delta} \times \frac{\delta}{R_0} = -\frac{\delta}{c_1} + \frac{c\delta}{c_1 c_3 R_0}$$

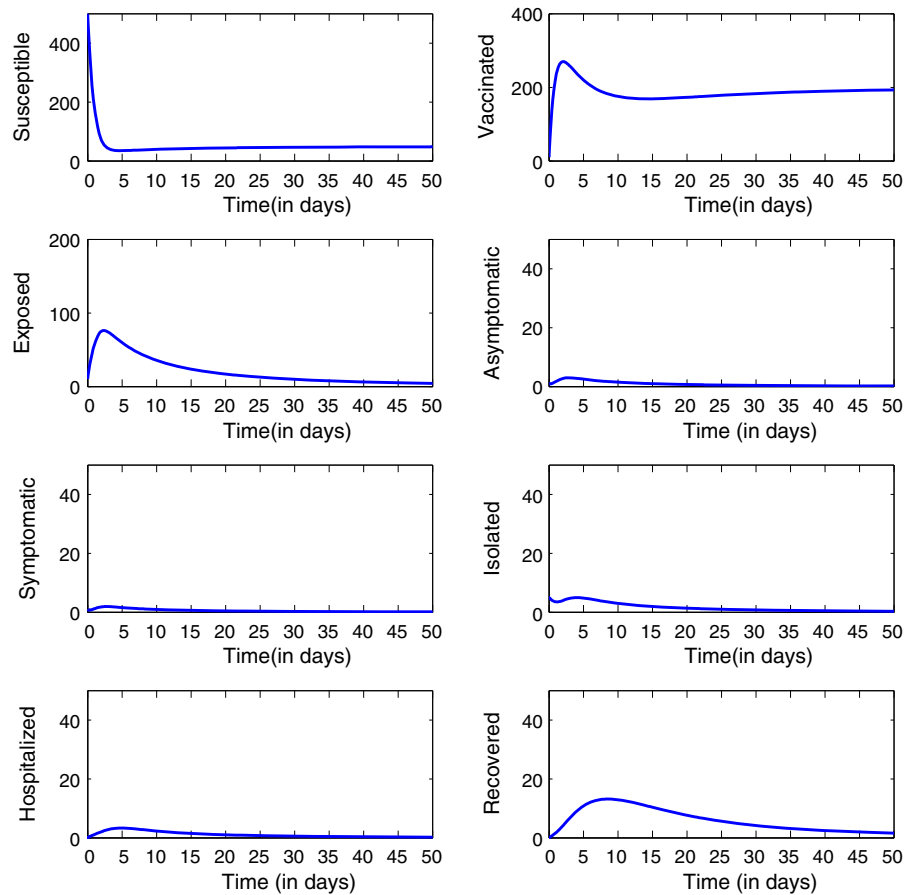
$$\Gamma_{\theta}^{R_0} = \frac{\partial R_0}{\partial \theta} \times \frac{\theta}{R_0} = -\frac{\epsilon c}{c_2^2 c_1} \times \frac{\theta}{R_0}$$

$$\Gamma_{\eta_a}^{R_0} = \frac{\partial R_0}{\partial \eta_a} \times \frac{\eta_a}{R_0} = -\frac{\epsilon c}{c_2^2 c_1} \times \frac{\rho_a}{R_0}$$

$$\Gamma_{\kappa}^{R_0} = \frac{\partial R_0}{\partial \kappa} \times \frac{\kappa}{R_0} = -\frac{\delta c}{c_1 c_3^2} \times \frac{\kappa}{R_0}$$

$$\Gamma_{\lambda}^{R_0} = \frac{\partial R_0}{\partial \lambda} \times \frac{\lambda}{R_0} = -\frac{\delta c}{c_3^2 c_1} \times \frac{\lambda}{R_0}$$

Fig. 3 Simulation results of model (1), when $R_0 > 1$



$$\begin{aligned} \Gamma_{\eta_i}^{R_0} &= \frac{\partial R_0}{\partial \eta_i} \times \frac{\eta_i}{R_0} = -\frac{\delta c}{c_3^2 c_1} \times \frac{\eta_i}{R_0} & \left(\frac{\epsilon}{c_2} + \frac{\delta}{c_3} \right) - \frac{c}{c_1 \left(\frac{\epsilon}{c_2} + \frac{\delta}{c_3} \right) \times \frac{d}{R_0}} \\ \Gamma_{\rho_i}^{R_0} &= \frac{\partial R_0}{\partial \rho_i} \times \frac{\rho_i}{R_0} = -\frac{\delta c}{c_3^2 c_1} \times \frac{\rho_i}{R_0} \\ \Gamma_{\beta}^{R_0} &= \frac{\partial R_0}{\partial \beta} \times \frac{\beta}{R_0} = 1 \\ \Gamma_{\Pi}^{R_0} &= \frac{\partial R_0}{\partial \Pi} \times \frac{\Pi}{R_0} = 1 \\ \Gamma_{\xi}^{R_0} &= \frac{\partial R_0}{\partial \xi} \times \frac{\xi}{R_0} = \frac{\alpha u \xi}{\xi \alpha u + d} \\ \Gamma_{\alpha}^{R_0} &= \frac{\partial R_0}{\partial \alpha} \times \frac{\alpha}{R_0} = \frac{\alpha (\xi - 1) u d}{(\xi \alpha u + d)(\alpha u + d)} \\ \Gamma_u^{R_0} &= \frac{\partial R_0}{\partial u} \times \frac{u}{R_0} = \frac{u (\xi - 1) \alpha d}{(\xi \alpha u + d)(\alpha u + d)}, \text{ and} \\ \Gamma_d^{R_0} &= \frac{\partial R_0}{\partial d} \times \frac{d}{R_0} \\ &= \frac{c_1 \beta \Pi}{d^2 (\alpha u + d)^2} \{ d(\alpha u + d) - (\xi \alpha u + d)(\alpha u + 2d) \} - c \\ & \qquad \qquad \qquad c_1^2 \end{aligned}$$

Table 2 contains the sensitivity indices for the basic reproduction number R_0 for the values of parameters in Table 1.

From Table 2, it is clear that the most sensitive parameters for the basic reproduction number R_0 of model 1 are Π, β, α and u . The positive index indicates that R_0 is an increasing function of the relevant parameter, while the negative index indicates that R_0 is a decreasing function of the relevant parameter. For example, $\Gamma_{\beta}^{R_0} = 1$, means that if we increase the parameter β by some percentage, then R_0 is also increased with the same percentage. Additionally, a rise in the value of ϵ will result 36.84% increase in the basic reproduction number. In contrast, increasing the value of α reduces R_0 by 76.30 %. As shown in Table 1, Π and β have a greater positive effect on R_0 than ϵ, δ, ξ

Table 2 The sensitivity index was calculated for the parameter values given in Table 1

Parameter symbols	Sensitivity indices
Π	1
β	1
ϵ	0.3684
δ	0.1721
ξ	0.0389
α	-0.7630
u	-0.7630
d	-0.6199
θ	-0.2582
η_a	-0.1631
ρ_a	-0.1359
κ	-0.1109
λ	-0.1047
η_i	-0.0986
ρ_i	-0.0493

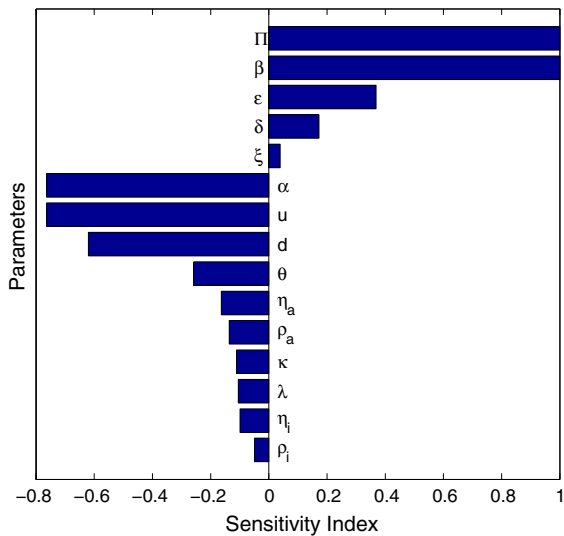


Fig. 4 The sensitivity index of R_0 against the concerning parameters

and α and u have a greater negative effect on R_0 than the remaining parameters affecting R_0 .

The results shown in Table 2 are depicted in Fig. 4. This figure demonstrates that parameters with a right-hand sidebar have a positive effect on, R_0 , whereas parameters with a left-hand sidebar have a negative effect, as well as longer the bar, the greater the sensitivity of R_0 for that parameter.

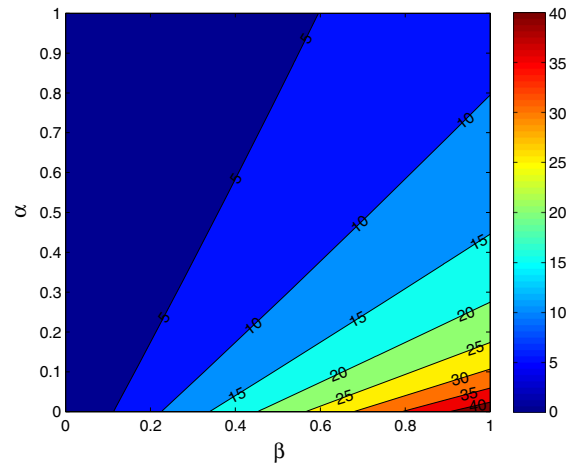


Fig. 5 Contour plots indicating nature of change in basic reproduction number (R_0) of model (1) under parametric planes. Contour Plot of R_0 as a function of α and β

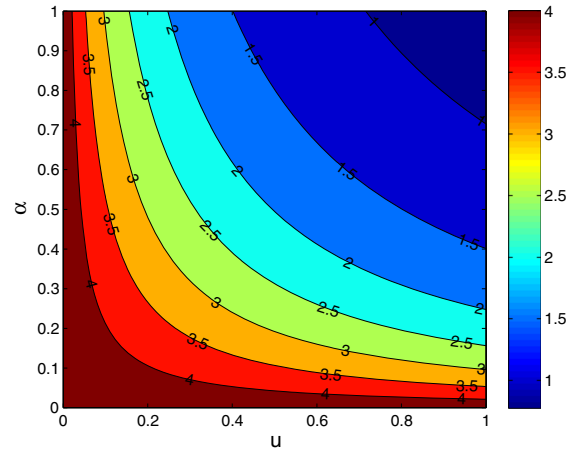


Fig. 6 Contour plots indicating nature of change in basic reproduction number (R_0) of model (1) under parametric planes. The Contour Plot of R_0 as a function of α and u

Figures 5 and 6 show the contour plots of the basic reproduction number R_0 with respect to the parameters α vs β and α vs u , respectively. As illustrated in Fig. 5, when β increases and α decreases then R_0 will increase. Thus, in order to control the ongoing COVID-19 pandemic, the basic reproduction number, R_0 , must be lowered, for which we must take measures to increase the value of α and to slow the disease transmission rate β . As seen in Fig. 6, when the control parameter u and the vaccination parameter α increases then R_0 falls. By increasing the value of the control parameter u , the

number of persons vaccinated increases and the rate of vaccination increases as well.

We know that the basic reproduction number, R_0 , therefore, in order to control the dynamics of disease transmission, we must reduce the value of R_0 . As a result of Table 2 and Figs. 4, 5 and 6, we can conclude that parameters with negative indices can be increased in order to significantly reduce R_0 . Additionally, we can observe that parameters such as Π , and β have positive indices, implying that by lowering their values, we can lower R_0 . As a consequence, we can control disease transmission in this manner.

5.3 Bifurcation diagram

In order to examine disease-free equilibria in system (1), Theorem 2 demonstrates that system (1) may undergo a transcritical bifurcation at the threshold parameter condition $R_0 = 1$. It has been discovered that system (1) exhibits a transcritical bifurcation when $R_0 = 1$, which is seen in Fig. 7. The locally stable equilibria are shown by solid blue lines, whereas the unstable equilibria are represented by dashed red lines. As the disease-free equilibrium is locally asymptotically stable for $R_0 < 1$, a solid blue line represents it. The disease-free equilibrium is unstable if $R_0 > 1$, and it is depicted as a red dashed line on the graph.

5.4 Numerical simulation of the optimal control problem

We now conduct a numerical simulation of the formulated optimum control problem. Using the forward fourth-order R-K technique, we begin by finding the numerical solution of system (1) using the initial values specified in Table 2. Then, utilising the numerical solution of the system and the transversality conditions, we apply the backward fourth-order R-K technique to determine the numerical solution of the system of adjoint equations.

We take the parametric values the same as in Table 1 except for $\alpha = 0.5$ and keep the same set of initial values. For numerical simulation, we take $b_1 = 1.2$, $b_2 = 1.2$, $b_3 = 1$. Fig. 8 represents the dynamics of populations of all the classes in the presence and absence of an optimal control strategy. From Fig. 8, we can see that in the absence of a control strategy, the population of

the susceptible and the vaccinated classes goes down faster than a control strategy. In the absence of vaccination, the populations of the remaining classes other than the isolated class increase then decrease exponentially and get flattered after some time. When vaccination is there, then the population of the classes increases slowly. In the absence of vaccination, the population of the infected class increases and then decreases exponentially after that gets flattered, but in the presence of vaccination strategy, the infected class goes down slowly.

In Fig. 9, we plotted the solution of the system of adjoint Eq. 4. Fig. 9 shows the variation in the evaluation of adjoint variables when the optimal control is applied to the proposed model. In Fig. 10, we plotted the variation in the optimal control parameter $u(t)$. We noticed in Fig. 10 that we initially keep a high vaccination rate for controlling the disease transmission and then decrease it gradually such that implementation cost is also minimised. This phenomenon is justified because as more and more populations are vaccinated, immunity against the virus also develops naturally in public, so we can gradually decrease the vaccination rate.

5.5 Parameter estimation-model fitting and model validation

The period from March 25, 2020, to April 24, 2020, is considered for model fitting. In India, we have accumulated daily cases of COVID-19 for this analysis. Cumulative COVID-19 cases were acquired from reference [29]. Model (1) is calibrated for India's cumulative daily cases. We enumerated the principal model parameters determined from data, in Table 3. The data will also estimate some of the initial conditions of model (1). Fitting cumulative daily cases in MATLAB is accomplished with the least-square function *fmincon*. Tables 3 and 4 list the parameters and initial conditions calculated using the approach described above. The daily cumulative reported cases of India are fitted and displayed in Fig. 11.

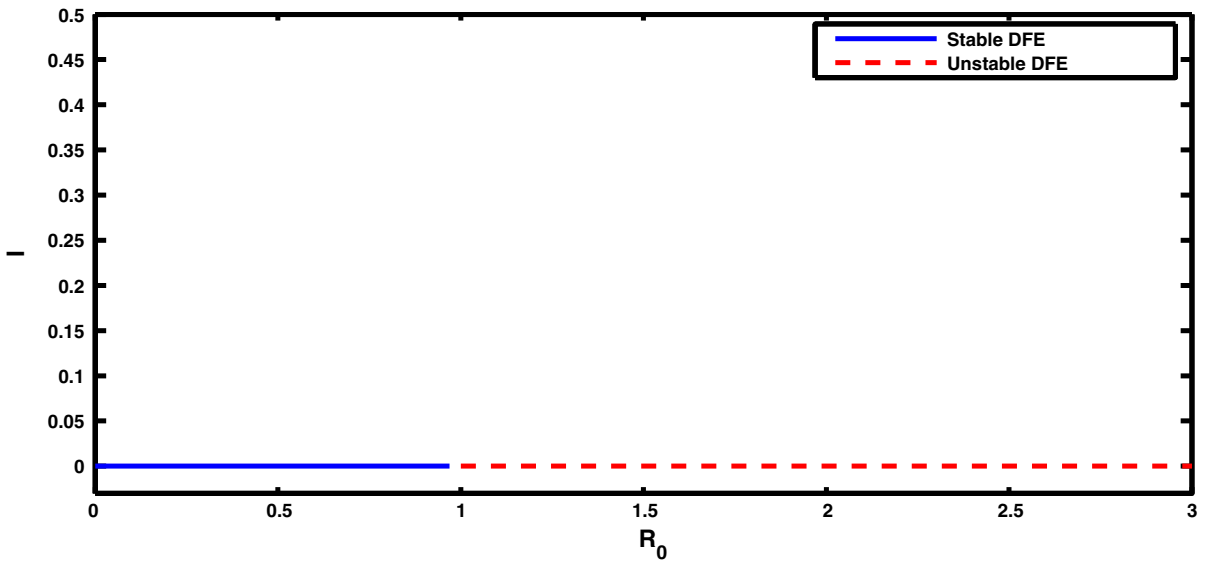


Fig. 7 The transcritical bifurcation diagram shows the behaviour of stability of disease-free equilibrium around R_0 . Here, solid blue line depicts stability state and red dashed line depicts instability

Fig. 8 Dynamics of classes in presence and absence of vaccination strategy

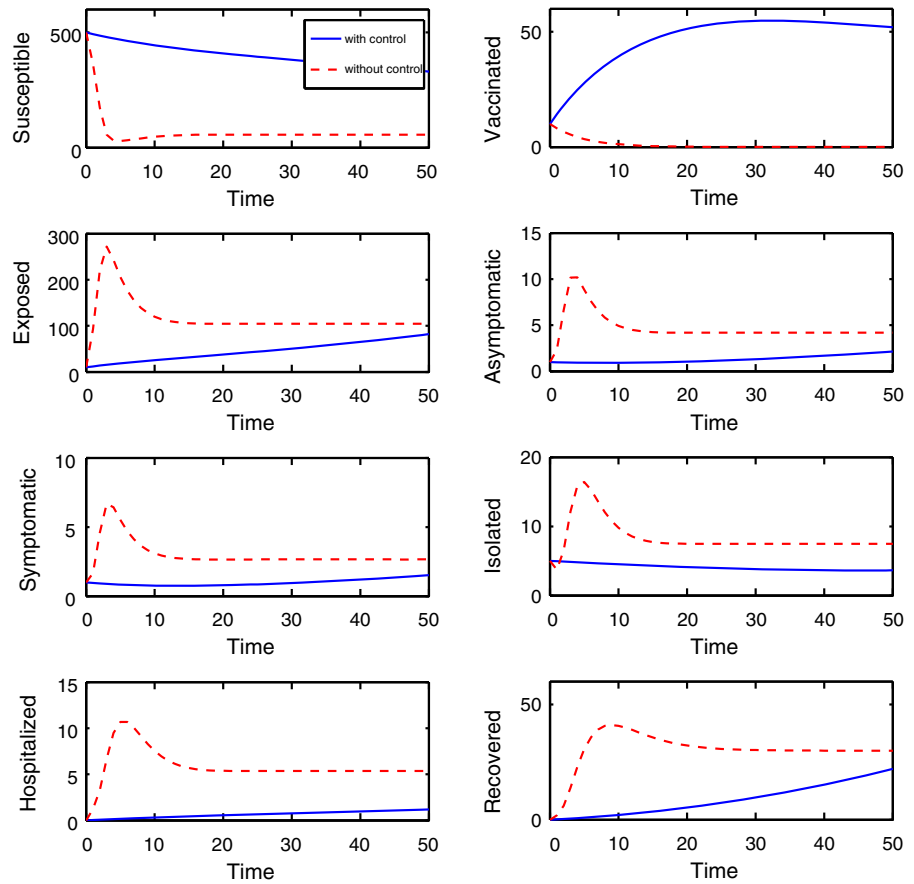


Fig. 9 Dynamics of the adjoint variables when control applied optimally

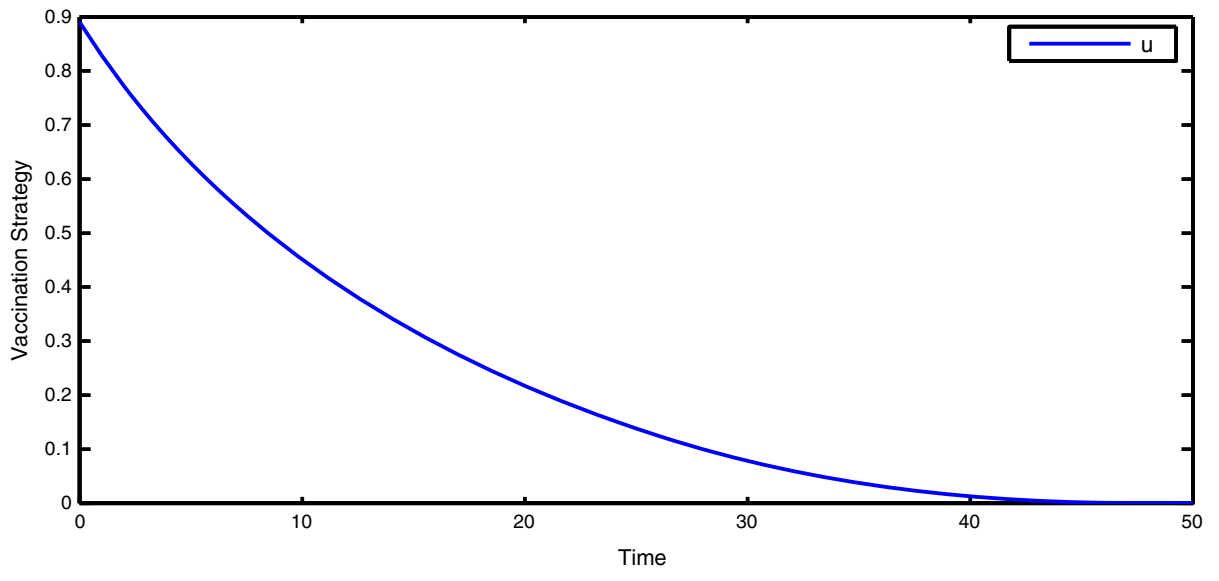
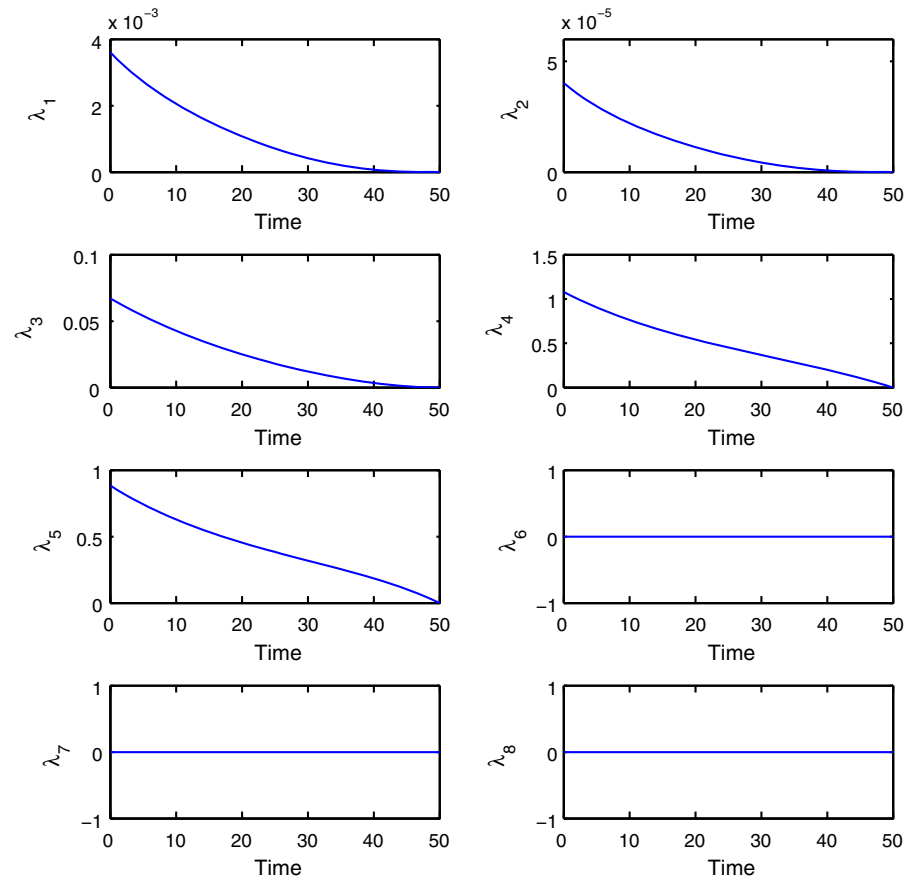


Fig. 10 Dynamics of the vaccination strategy

Table 3 Estimated values of the parameters used in model (1) through model fitting technique

Parameters	Value	Source
Π	67446.82	[30]
α	0.99879	Estimated
β	0.00001	Estimated
ξ	0.00001	Estimated
d	0.0000391	[30]
ϵ	0.00064	Estimated
δ	0.62	[31]
θ	0.95879	Estimated
κ	0.98784	Estimated
λ	0.8576	Estimated
μ	0.2756	Estimated
η_a	0.6987	Estimated
η_i	0.8789	Estimated
η_j	0.2548	Estimated
η_h	0.2579	Estimated
ρ_a	0.73	[31]
ρ_i	0.79	[31]
ρ_j	0.4786	Estimated
ρ_h	0.8368	[32]
u	0.995	Assumed

Table 4 Estimated initial population size for India

Parameters	Value	Source
$S(0)$	1352642280	[30]
$\mathcal{V}(0)$	0	Assumed, since no vaccination started till that time
$\mathcal{E}(0)$	1302	Estimated
$\mathcal{A}(0)$	479	Estimated
$\mathcal{I}(0)$	356	Estimated
$\mathcal{J}(0)$	657	[30]
$\mathcal{H}(0)$	657	[30]
$\mathcal{R}(0)$	452	Estimated

We validate the model by comparing the model prediction with the reported data. We compared the daily

cases predicted by the algorithm from April 25, 2020, to May 10, 2020. Fig. 12 depicts the model prediction scenarios estimated from the set of parameters and initial values from Tables 3 and 4, respectively.

6 Conclusion

This study modified the SEIR model to include eight infection classes and vaccination as a control parameter in order to simulate and predict the spread of a novel coronavirus disease. To begin, mathematical analysis was used to demonstrate the positivity and boundedness, disease-free equilibrium, and basic reproduction number of the suggested model. In the second step, The qualitative dynamic behaviour of the model was explored, and the basic reproduction number, R_0 , was calculated using the next-generation matrix approach. The result indicates that the model is asymptotically stable at infection-free equilibrium for $R_0 < 1$ and unstable for $R_0 > 1$. We analysed the optimum control issue and performed several numerical simulations on the solutions of the model. In addition, we performed sensitivity analysis and generated a bifurcation diagram. A simulation of the optimum control has been performed numerically. Validation and prediction of models are also performed.

Finally, we investigated the impact of vaccination on the spread of the disease and showed that a combination of community mitigation strategies and vaccination events could be effective measures to diminish coronavirus by minimising social and economic costs. Our analysis demonstrates that expanding the vaccination program considerably reduces the number of confirmed cases and deaths. The proposed model can be used to assist public health officials in planning, preparing, and implementing appropriate measures and decisions to control the pandemic.

Additionally, the models we presented contain a large number of parameters whose estimated values may be subjected to uncertainty. Thus, uncertainty analysis may be used to determine the parameters that have the largest impact on the chosen response function based on the numerical simulation results.

Fig. 11 Model (1) fitted to cumulated daily cases of India from April 25, 2020, to May 10, 2020. Here, observed data points are shown in red dots and the solid blue line depicts the model fitted curve

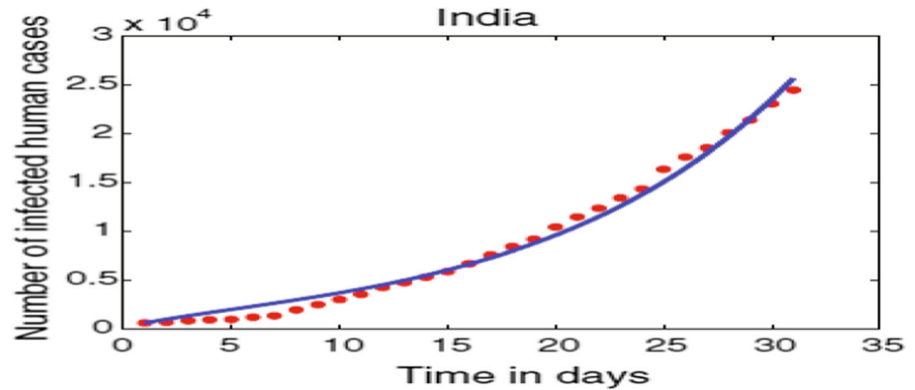
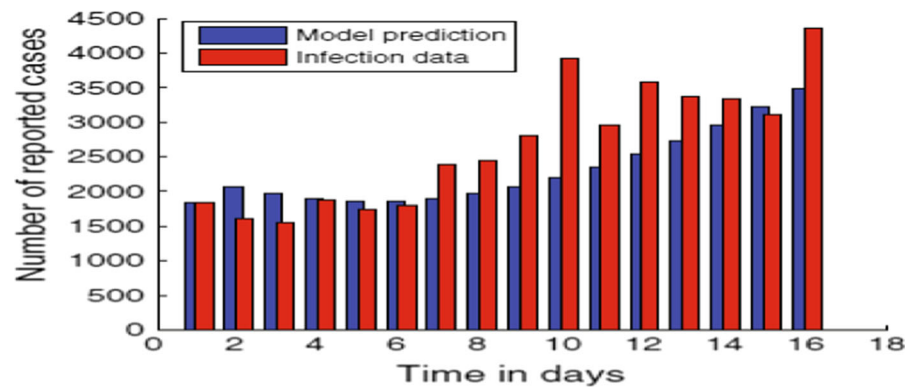


Fig. 12 The Bar graph of daily infected cases. The blue bar shows the model predicted cases and red bar depicts the observed cases



Author contributions All authors contributed to the study conception and design. All authors read and approved the final manuscript.

Funding The authors declare that no funds, grants, or other support were received during the preparation of this manuscript.

Data availability The datasets that analysed and support the findings of this study are available within the article.

Declarations

Conflict of interest The authors declare that they have no conflict of interest.

References

1. World Health Organization: Naming the coronavirus disease (COVID-19) and the virus that causes it (2020). [https://www.who.int/emergencies/diseases/novel-coronavirus-2019/technical-guidance/naming-the-coronavirus-disease-\(covid-2019\)-and-the-virus-that-causes-it](https://www.who.int/emergencies/diseases/novel-coronavirus-2019/technical-guidance/naming-the-coronavirus-disease-(covid-2019)-and-the-virus-that-causes-it). Accessed 15 Sep 2021
2. WHO Director-General's opening remarks at the media briefing on COVID-19 - 11 March 2020 (2020). <https://www.who.int/director-general/speeches/detail/who-director-general-s-opening-remarks-at-the-media-briefing-on-covid-19---11-march-2020>. Accessed 15 Sep 2021
3. World Health Organization: Coronavirus (COVID-19) dashboard (2021). <https://covid19.who.int/>. Accessed 18 Sep 2021
4. NCBI: First confirmed case of COVID-19 infection in India: a case report. <https://www.ncbi.nlm.nih.gov/pmc/articles/PMC7530459/>. Accessed 15 Sep 2021
5. World Health Organization: Coronavirus Disease (COVID-19) Dashboard With Vaccination Data - India (2021). URL <https://covid19.who.int/region/searo/country/in>. Accessed 18 Sep 2021
6. Kermack, W., Mckendrick, A.: A contribution to the mathematical theory of epidemics. *Am. Math. Mon.* **45**(7), 446 (1938). <https://doi.org/10.2307/2304150>
7. Kermack, W., Mckendrick, A.: Contributions to the mathematical theory of epidemics—I. *Bull. Math. Biol.* **53**(1–2), 33–55 (1991). <https://doi.org/10.1007/BF02464423>

8. Soni, R., Chouhan, U.: A dynamic effect of infectious disease on prey predator system and harvesting policy. *Biosci. Biotechnol. Res. Commun.* **11**, 231–237 (2018)
9. Buonomo, B., D’Onofrio, A., Lacitignola, D.: Global stability of an SIR epidemic model with information dependent vaccination. *Math. Biosci.* **216**(1), 9–16 (2008). <https://doi.org/10.1016/j.mbs.2008.07.011>
10. Jana, S., Haldar, P., Kar, T.K.: Optimal control and stability analysis of an epidemic model with population dispersal. *Chaos, Solitons Fractals* **83**, 67–81 (2016). <https://doi.org/10.1016/j.chaos.2015.11.018>
11. Jana, S., Nandi, S.K., Kar, T.K.: Complex dynamics of an SIR epidemic model with saturated incidence rate and treatment. *Acta. Biotheor.* **64**(1), 65–84 (2016). <https://doi.org/10.1007/s10441-015-9273-9>
12. Li, L., Wang, C.H., Wang, S.F., Li, M.T., Yakob, L., Cazelles, B., Jin, Z., Zhang, W.Y.: Hemorrhagic fever with renal syndrome in China: mechanisms on two distinct annual peaks and control measures. *Int. J. Biomath.* **11**(2), 1850030 (2018). <https://doi.org/10.1142/S1793524518500304>
13. Acuña-Zegarra, M.A., Olmos-Liceaga, D., Velasco-Hernández, J.X.: The role of animal grazing in the spread of Chagas disease. *J. Theor. Biol.* **457**, 19–28 (2018). <https://doi.org/10.1016/j.jtbi.2018.08.025>
14. Avilov, K.K., Romanyukha, A.A., Borisov, S.E., Belilovsky, E.M., Nechaeva, O.B., Karkach, A.S.: An approach to estimating tuberculosis incidence and case detection rate from routine notification data. *Int. J. Tuberc. Lung Dis.* **19**(3), 288–294 (2015). <https://doi.org/10.5588/ijtld.14.0317>
15. Jiang, S., Wang, K., Li, C., Hong, G., Zhang, X., Shan, M., Li, H., Wang, J.: Mathematical models for devising the optimal Ebola virus disease eradication. *J. Transl. Med.* **15**(1), 124 (2017). <https://doi.org/10.1186/s12967-017-1224-6>
16. Carvalho, S.A., Silva, S.O., Charret, Id.C.: Mathematical modeling of dengue epidemic: control methods and vaccination strategies. *Theory Biosci.* **138**(2), 223–239 (2019). <https://doi.org/10.1007/s12064-019-00273-7>
17. Ndaïrou, F., Area, I., Nieto, J.J., Torres, D.F.M.: Mathematical modeling of COVID-19 transmission dynamics with a case study of Wuhan. *Chaos, Solitons Fractals* **135**, 109846 (2020). <https://doi.org/10.1016/j.chaos.2020.109846>
18. Mandal, M., Jana, S., Kumar, S., Khatua, A., Adak, S., Kar, T.K.: A model based study on the dynamics of COVID-19: prediction and control. *Chaos, Solitons Fractals* **136**, 109889 (2020). <https://doi.org/10.1016/j.chaos.2020.109889>
19. Prathumwan, D., Trachoo, K., Chaiya, I.: Mathematical modeling for prediction dynamics of the Coronavirus disease 2019 (COVID-19) pandemic, quarantine control measures. *Symmetry* **12**(9), 1404 (2020). <https://doi.org/10.3390/SYM12091404>
20. Biswas, S.K., Ghosh, J.K., Sarkar, S., Ghosh, U.: COVID-19 pandemic in India: a mathematical model study. *Nonlinear Dyn.* **102**(1), 537–553 (2020). <https://doi.org/10.1007/s11071-020-05958-z>
21. Gumel, A.B., Iboi, E.A., Ngonghala, C.N., Elbasha, E.H.: A primer on using mathematics to understand COVID-19 dynamics: modeling, analysis and simulations. *Infect. Dis. Model.* **6**, 148–168 (2021). <https://doi.org/10.1016/j.idm.2020.11.005>
22. Ghostine, R., Gharamti, M., Hassrouny, S., Hoteit, I.: An extended SEIR model with vaccination for forecasting the COVID-19 Pandemic in Saudi Arabia using an ensemble Kalman filter. *Mathematics* **9**(6), 636 (2021). <https://doi.org/10.3390/math9060636>
23. Das, P., Upadhyay, R.K., Misra, A.K., Rihan, F.A., Das, P., Ghosh, D.: Mathematical model of COVID-19 with comorbidity and controlling using non-pharmaceutical interventions and vaccination. *Nonlinear Dyn.* **106**(2), 1213–1227 (2021). <https://doi.org/10.1007/s11071-021-06517-w>
24. Das, P., Nadim, S.S., Das, S., Das, P.: Dynamics of COVID-19 transmission with comorbidity: a data driven modelling based approach. *Nonlinear Dyn.* **106**, 1197–1211 (2021). <https://doi.org/10.1007/s11071-021-06324-3>
25. Yu, X., Qi, G., Hu, J.: Analysis of second outbreak of COVID-19 after relaxation of control measures in India. *Nonlinear Dyn.* **106**, 1149–1167 (2021). <https://doi.org/10.1007/s11071-020-05989-6>
26. Hu, J., Qi, G., Yu, X., Xu, L.: Modeling and staged assessments of the controllability of spread for repeated outbreaks of COVID-19. *Nonlinear Dyn.* **106**, 1411–1424 (2021). <https://doi.org/10.1007/s11071-021-06568-z>
27. Xin, H., Li, Y., Wu, P., Li, Z., Lau, E.H.Y., Qin, Y., Wang, L., Cowling, B.J., Tsang, T.K., Li, Z.: Estimating the latent period of coronavirus disease 2019 (COVID-19). *Clin. Infect. Dis.* **74**(9), 1678–1681 (2021). <https://doi.org/10.1093/cid/ciab746>
28. Van Den Driessche, P., Watmough, J.: Reproduction numbers and sub-threshold endemic equilibria for compartmental models of disease transmission. *Math. Biosci.* **180**(1–2), 29–48 (2002). [https://doi.org/10.1016/S0025-5564\(02\)00108-6](https://doi.org/10.1016/S0025-5564(02)00108-6)
29. Worldometer: COVID-19 CORONAVIRUS PANDEMIC (2022). <https://www.worldometers.info/coronavirus/country/india/>. Retried 09 May 2022
30. Central Intelligence Agency: India - The World Factbook - CIA. <https://www.cia.gov/the-world-factbook/countries/india/people-and-society>. Retrieved 09 May 2022
31. Sardar, T., Nadim, S., Rana, S., Chattopadhyay, J.: Assessment of lockdown effect in some states and overall India: a predictive mathematical study on COVID-19 outbreak. *Chaos Solitons Fractals* (2020). <https://doi.org/10.1016/j.chaos.2020.110078>
32. India covid-19 tracker (2022). URL <https://www.covid19india.org/>. Retrieved 09 May 2022

Publisher’s Note Springer Nature remains neutral with regard to jurisdictional claims in published maps and institutional affiliations.